

EFFECT OF BIOFILM FORMATION ON THE AGGREGATION OF MICROPLASTICS IN UPPER-OCEAN TURBULENCE

F. Pizzi¹, M. Rahmani², C. Romera-Castillo³, F. Peters³, J. Grau¹, F. Capuano¹, L. Jofre¹

¹ *Dept. Fluid Mechanics, Universitat Politècnica de Catalunya, Spain*

² *Dept. Chemical & Biological Engineering, University of British Columbia, Canada*

³ *Dept. Marine Biology & Oceanography, Institut de Ciències del Mar - CSIC, Spain*

lluis.jofre@upc.edu

Abstract

The impact of biofilm formation on marine microplastics in the upper layers of the ocean has been investigated using direct numerical simulations with an Eulerian-Lagrangian point-particle approach. The influence of biofilm is modeled through the coalescence efficiency, also known as the stickiness parameter, which quantifies the probability of aggregation after a collision event. The results indicate that, owing to the small size of the particles, both microplastics and biogenic debris essentially behave as tracers, following the fluid flow. Differences in features such as aggregates formation and preferential concentration weakly depend on the tendency of aggregation. While this model simplifies the actual conditions of biofouled microplastics in the ocean, it provides a robust foundation for future numerical and experimental studies.

1 Introduction

The distribution and impact of marine microplastics (MPs) is a growing concern in the field of environmental science and marine biology [Clark et al. (2016)]. The term microplastic refers to small plastic particles (and eventually residuals) which are characterized by sizes smaller than 5 millimeters [Eriksen et al. (2014)] and they have accumulated in oceans and other bodies of water. They can come from a variety of sources including discarded plastic products, fibers from clothing and textiles, and microbeads from personal care products [Bashir et al. (2021)]. In particular, their presence and interaction with flora and fauna have significant impacts on oceanic ecosystems. For example, plastic particles can be ingested by fish and other marine organisms, potentially leading to internal injuries and other health issues [Eerkes-Medrano et al. (2015)]. Additionally, the accumulation of microplastics in ocean can contribute to the degradation of marine habitats, and can even enter the human food chain through the consumption of seafood.

Despite the growing awareness of the negative impacts of marine MPs, the full extent of its distribution and influence on marine environments remains largely unknown. In this regard, research efforts are ongoing to better understand the sources, distribution, and ef-

fects of MPs in marine ecosystems, with the ultimate goal of finding ways to mitigate their consequences on both marine life and human health [Eerkes-Medrano et al. (2015)]. Out of the 8 metric tons of plastic entering the ocean every year on average, only 1% have been found and counted floating in the surface [Van Sebille et al. 2015]. One of the fates of that called “missing plastic” is thought to be sinking to the deep ocean sediments [Woodall et al. (2014)]. However, the transportation and fate of MPs in oceanic environments is far from trivial as a result of the presence of turbulence flow motions and the interaction between themselves and with biogenic entities, which can eventually result in the formation of aggregates of different sizes and compositions. Despite their small size and lower density compared to water, recent hypotheses suggest that MPs can settle from the surface to deeper layers and disperse throughout the entire ocean by aggregating with biogenic particles (BP). These biogenic particles include living and dead zooplankton and phytoplankton. The aggregation processes are highly influenced by the formation and characteristics of biofilms covering the MPs and biogenic particles. In detail, biofilms are formed of complex communities of microorganisms which have significant impact on the physical and chemical properties of MPs [Kooi et al. (2017)]. Specifically, the accumulation of biofilm on marine MPs may change their buoyancy, toxicity, “stickiness” and persistence in the marine environment. Moreover, biofilms can serve as a habitat for diverse microbial communities, facilitating the transfer of harmful bacteria and other microorganisms between marine organisms and ecosystems [Michels et al. (2018)]. Therefore, understanding the formation and development of biofilms on marine MPs is crucial because it is the first step toward developing effective strategies to mitigate their impact on ecosystems and human health.

The scientific community is tackling this challenge by investigating the factors that influence biofilm formation and growth on microplastics, such as water chemistry, microbial community composition, the physical and chemical properties of the plastics themselves, and the flow conditions. However, there is no common agreement regarding the effects of turbulence

on the biofilm dynamics [Takeuchi et al. (2019), Moreira et al. (2013), Teodosio et al. (2011)]. The core of the problem is the antagonistic effects of shear stresses (which increase with turbulent intensity) that enhance the diffusion of nutrients but, at the same time, erode the biofilm by means of mechanical stresses. Moreover, the presence of biofilm can also affect the turbulent flow dynamics by altering the surface roughness and hydrodynamic drag of the underlying substrate. This complex interplay between turbulent flow and biofilms has important implications, the better understanding of which can lead to developing more effective strategies to prevent and mitigate the impact of microplastic-biofilms on aquatic ecosystems and human health. In this context, Figure 1 offers a visual representation of the aforementioned discussion. This aggregation phenomenon plays a significant role in the transport and distribution of MPs in marine environments. In particular, the movement of MP particles follows a complex and multifaceted process that depends on several factors: (i) their initial characteristics, including density, size, and shape; (ii) oceanic flow conditions like wind, waves, currents, and turbulence; and (iii) the mechanisms of aggregation with BPs. In this regard, the paper is organized as follows. First, Section 2 presents the mathematical framework utilized to describe fluid flow and discrete phase. Next, Section 3 presents the results and their discussion. Finally, in Section 4, the conclusions, implications, and possible future studies are reported.

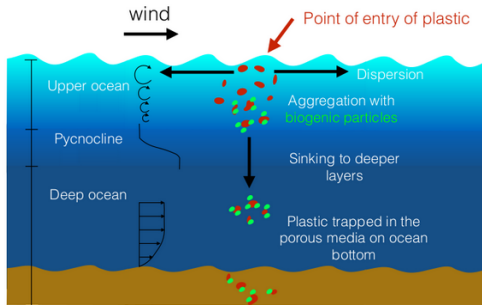


Figure 1: Schematic representation of the main processes governing the fate of microplastics in oceans.

2 Physics modeling

The problem of marine MPs can be considered as a paradigm of particle-laden turbulence, where a fluid flow (carrier) contains solid particles (dispersed phase) suspended within it. The behavior of this flow can be described mathematically using various approaches, such as continuum models, kinetic theory, or particle-based simulations [Subramaniam (2013)]. In the present analysis, the so-called Lagrangian-Eulerian approach (LE) is utilized. In this scenario, the dispersed phase is described as a stochastic phenomenon in a Lagrangian system, while the carrier phase is considered in an Eulerian frame. To conduct

| MP | | BP | |
|---------------------|---------------------|---------------------|---------------------|
| d_{p_1} [m] | St_1 | d_{p_2} [m] | St_2 |
| $1.5 \cdot 10^{-4}$ | $1.9 \cdot 10^{-4}$ | $7.5 \cdot 10^{-5}$ | $2.0 \cdot 10^{-5}$ |

Table 1: Microplastic and biogenic particles considered.

the study, direct numerical simulations (DNS) with a point-particle approach [Jofre et al. (2020)] is employed. This choice is motivated by the fact that particle dimensions are smaller than the smallest flow scale (Kolmogorov scale). Despite the computationally expensive nature of DNS, they allow for the complete resolution of the flow field and the particle interactions. As a result, DNS provides valuable insights into the intricate dynamics of particle-laden turbulence.

The flow field is described by means of the following dimensionless conservation equations for mass and momentum [Jofre et al. (2020)]

$$\nabla \cdot \mathbf{u}_f = 0, \quad (1)$$

$$\frac{\partial \mathbf{u}_f}{\partial t} + \nabla \cdot (\mathbf{u}_f \otimes \mathbf{u}_f) = -\nabla p + \frac{1}{Re_\lambda} \Delta \mathbf{u}_f + \mathbf{f}_{\text{TWC}}, \quad (2)$$

where \mathbf{u}_f and p are the dimensionless fluid velocity and pressure. $Re_\lambda = U_{rms} \lambda / \nu_f$ is the Taylor Reynolds number with U_{rms} the root-mean-square velocity fluctuations, λ the Taylor microscale, and $\nu_f = \mu_f / \rho_f$ the kinematic viscosity, and μ_f and ρ_f the dynamic viscosity and density of the fluid, respectively. Additionally, \mathbf{f}_{TWC} is a two-way coupling term that accounts for the effect of particle forces on the fluid, which is defined as

$$\mathbf{f}_{\text{TWC}} = \sum_{k=1}^{N_s} \frac{\Phi_{m_k}}{St_{\lambda_k} N_{p_k}} \sum_{p=1}^{N_{p_k}} (\mathbf{v}_p - \mathbf{u}_p) \delta(\mathbf{x} - \mathbf{x}_p), \quad (3)$$

with \mathbf{u}_p representing the dimensionless fluid velocity at particle locations, N_s denoting the number of particle classes, and $\delta(\mathbf{x} - \mathbf{x}_p)$ as the Dirac delta function concentrated at the particle positions \mathbf{x}_p . In the simulations conducted for this study, \mathbf{f}_{TWC} was found to be substantially small. The flow and particle relaxation times are defined as $\tau_\lambda = \lambda / U_{rms}$ and $\tau_p = \rho_p d_p^2 / (18 \mu_f)$, respectively, where ρ_p and d_p are the density and diameter of particles. By calculating the Stokes number $St_\lambda = \tau_p / \tau_\lambda$ based on these timescales, the response time of particles with respect to the flow can be characterized. Finally, $\Phi_m = \rho_p \Phi_v / \rho_f$ represents the mass fraction of particles in the fluid, where $\Phi_v = N_p m_p / (\rho_p \lambda^3)$ is the corresponding volume fraction. In connection to these dimensionless numbers, the Reynolds number considered for this work is $Re_\lambda = 60$, and Table 1 summarizes the Stokes values considered.

Lagrangian Representation of Particles

One of the main hypotheses of this work is that particle (and aggregate) diameters d_p are significantly smaller than the Kolmogorov flow scale $\eta = \lambda / \sqrt{15}$,

i.e., $d_p/\eta \ll 1$. Moreover, the study of the settling velocity of particles \mathbf{v}_s is neglected since these are relatively small compared to U_{rms} . Additionally, the density ratio between particles and fluid is fixed at $\rho_p/\rho_f = 0.97$ for microplastics and $\rho_p/\rho_f = 1.17$ for biogenic. Particles are consequently modeled following a Lagrangian point-particle (PP) approach, in which Stokes' drag \mathbf{F}_D is the most important force [Maxey and Riley (1983)]. This assumption is asymptotically valid in the limit in which particles are dense compared to the fluid. Otherwise, the history force \mathbf{F}_H of particles needs to be considered. However, \mathbf{F}_H : (i) becomes significant only when $\rho_p/\rho_f < 10$ [Pumir et al. (2016)], (ii) has been reported to scale as $\|\mathbf{F}_H\|/\|\mathbf{F}_D\| \sim d_p/\eta$, and (iii) typically has relatively small impacts on the distribution of particles. As a result, the Stokes' drag is retained as the dominant force, and the description of particles in terms of dimensionless positions and velocities is given by

$$\frac{d\mathbf{x}_p}{dt} = \mathbf{v}_p, \quad (4)$$

$$\frac{d\mathbf{v}_p}{dt} = \frac{\mathbf{u}_p - \mathbf{v}_p}{St\lambda_k}. \quad (5)$$

Biofilm & Coalescence

This work aims to model the aggregation between particles by employing the concept of coalescence efficiency, often referred to as the stickiness parameter α [Burd and Jackson (2009)]. This parameter quantifies the propensity of particles in a fluid to adhere or stick to each other upon collision, and it represents the dimensionless probability of a collision leading to coalescence rather than bouncing or rebounding. The stickiness parameter is typically calculated based on various physical and chemical properties of the particles, such as their size, shape, and surface chemistry, along with the properties of the fluid, including viscosity and surface tension. In this study, to represent different scenarios of biofouled marine microplastics, the following three stickiness values are considered $\alpha = 0.33, 0.66, 1$. In this scenario a more developed biofilm is represented by higher stickiness and, ultimately, a higher tendency to coalescence. The hypothesis to maintain the α constant in time is supported by several experimental works which observe a pseudo steady state behavior of this parameter for several classes of biofilm [Kiorboe et al. (1990), Balakin et al. (2012)] The goal is to perform a sensitivity analysis to assess the impact of biofilms on statistical features. Therefore, by investigating various stickiness scenarios, insight can be gained regarding the aggregation behavior in particle-laden flows, and explore how different biofilm-covered MPs may interact and affect the overall dynamics of the system.

3 Results & Discussion

The first analysis performed in this study focuses on the radial distribution function (RDF), which is

a measure used to describe the spatial arrangement and distribution of particles around a reference particle. The RDF provides valuable insights into particle-particle interactions and enables to quantify the probability of finding a particle at a specific distance from a reference particle, normalized by the expected probability in a homogeneous random distribution. Mathematically, the RDF is defined as follows

$$g(r) = \frac{N_r V}{V_r N}, \quad (6)$$

where the N_r represents the average number of particles located in a shell of volume V_r at a distance r from the reference particle. The volume of the sphere containing the total number of particle pairs is denoted by V . In this volume, the total number of particle pairs can be calculated as $N = M(M - 1)/2$, where M is the number of particles in the domain. To provide a clear understanding of the physical meaning, Figure 2 schematically illustrates the aforementioned concepts.

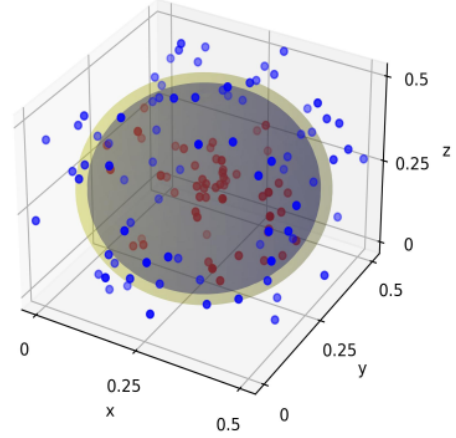


Figure 2: Illustration of the computational domain comprising the total cubic region, the spherical area where the RDF is computed (enclosed within the grey sphere of volume V), and the yellow shell representing the volume V_r .

In Figure 3, RDF normalized by particle radius is depicted for the three stickiness parameters at time $t/t_\lambda = 4$. In the top panel, it is observed the MP-MP RDF, which exhibits a standard shape with an asymptotic unitary value for $r_p/\langle r_p \rangle > 10$. This indicates that MPs do not show a preferential concentration with respect to each other. However, for BP, as shown in Figure 3(b), a clear peak is observed at $r_p/\langle r_p \rangle \approx 5$, indicating a slight concentration, especially for larger stickiness values. This observation is reasonable since higher stickiness enhances the coalescence tendency of particles, leading to their clustering. In contrast to the homogeneous distribution of microplastics among other microplastics, a preferential concentration of biogenic particles is evident, as depicted in Figure 3(c).

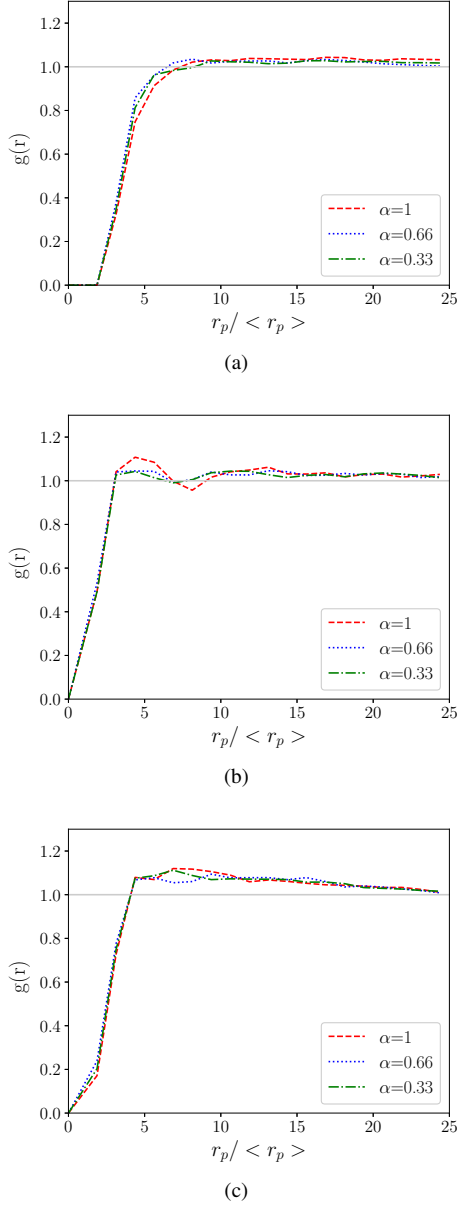


Figure 3: Radial distribution function for MP-MP (a) MP-BP (b) and BP-BP (c).

An additional useful tool for analyzing the probability of collision events is the joint probability density function (PDF) of the invariants of the velocity-gradient tensor of particles. Given that the Stokes number of the particles is significantly low, i.e., they act like tracers, the hypothesis that $\mathbf{u}_p \approx \mathbf{v}_p$ is utilized, meaning that particles follow the flow motion. The velocity-gradient tensor $A_{ij} \equiv \partial u_i / \partial x_j$ can be decomposed into symmetric and skew-symmetric parts, which respectively read

$$S_{ij} \equiv \frac{1}{2} \left(\frac{\partial u_i}{\partial x_j} + \frac{\partial u_j}{\partial x_i} \right), \quad (7)$$

and

$$\Omega_{ij} \equiv \frac{1}{2} \left(\frac{\partial u_i}{\partial x_j} - \frac{\partial u_j}{\partial x_i} \right). \quad (8)$$

Notice that $A_{ij} = S_{ij} + \Omega_{ij}$. The coefficients (P_A , Q_A , R_A) multiplying the eigenvalues λ_i of the characteristic equation of A_{ij} , satisfy the following relation

$$\lambda_i^3 + P_A \lambda_i^2 + Q_A \lambda_i + R_A = 0, \quad (9)$$

whose components explicitly are

$$P_A = -A_{ii} = -(S_{ii} + \Omega_{ii}) = 0, \quad (10)$$

$$Q_A = -\frac{1}{2} A_{ij} A_{ji} = -\frac{1}{2} (S_{ij} S_{ji} + \Omega_{ij} \Omega_{ji}), \quad (11)$$

$$R_A = -\frac{1}{3} A_{ij} A_{jk} A_{ki} = -\frac{1}{3} (S_{ij} S_{jk} S_{ki} + 3\Omega_{ij} \Omega_{jk} S_{ki}). \quad (12)$$

The results in terms of the second (Q_A) versus third (R_A) tensor invariants are presented in Figure 4 for two different stickiness parameters: $\alpha = 0.33$ and $\alpha = 1$. Interestingly, there are no substantial differences observed between the behavior of MPs and BPs, nor between the two different stickiness values. This behavior reflects the fact that the simulated regime is characterized by small Stokes numbers. Consequently, particles behave like tracers, resulting in the typical tear-shaped pattern shown in Figure 4. The similarity in their behavior indicates that both particle types are largely influenced by the underlying fluid flow, behaving in a similar manner, despite differences in their stickiness properties.

In Figure 5, the contour plot of the axial vorticity alongside the distribution of MPs (blue points) and aggregates (red points) are shown. Several notable features stand out: (i) particles tend to occupy regions of lower vorticity, in line with the theory that lighter particles have a preference for such regions; (ii) aggregates, on the other hand, are randomly scattered throughout the domain, indicating less influence from vorticity on their distribution; and (iii) the contour lines of the fluid flow exhibit varying magnitudes and shapes, suggesting that particles with different stickiness parameters have distinct impacts on the flow field. These observations offer valuable insights into the behavior and interactions of particles and aggregates within the flow, shedding light on the complex dynamics influenced by particle properties and the surrounding fluid environment.

The final analysis of this work focuses on the aggregates. In particular, Figure 6 shows the time evolution of the number of aggregates. It is interesting to observe that, regardless of the coalescence efficiency, the aggregates formed appear to be quite similar in composition, and constituting an extremely small percentage compared to the total number of initial particles. These findings reveal that aggregate formation is a relatively rare event. This suggests that in the simulated conditions, the aggregation process is limited, and individual particles mostly remain dispersed within the flow. Therefore, further investigation into the factors influencing aggregates formation could provide valuable insights into the dynamics of particle interactions and their impact on the overall system behavior.

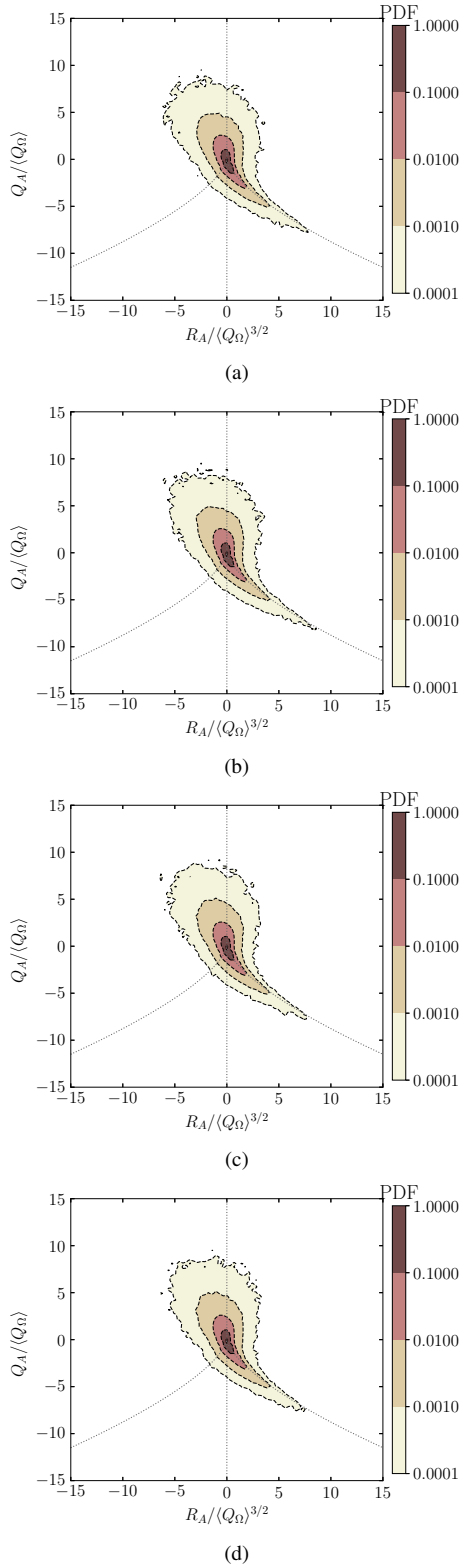


Figure 4: Joint PDFs for the second tensor invariant Q_A and third tensor invariant R_A at $t/\tau_\lambda = 4$. Utilizing $\alpha = 0.33$ for MPs (a) and BPs (b), and utilizing $\alpha = 1$ for (c) MPs and (d) BPs.

4 Conclusions & Perspectives

A preliminary study of the influence of biofilm formation, represented by the stickiness coefficient

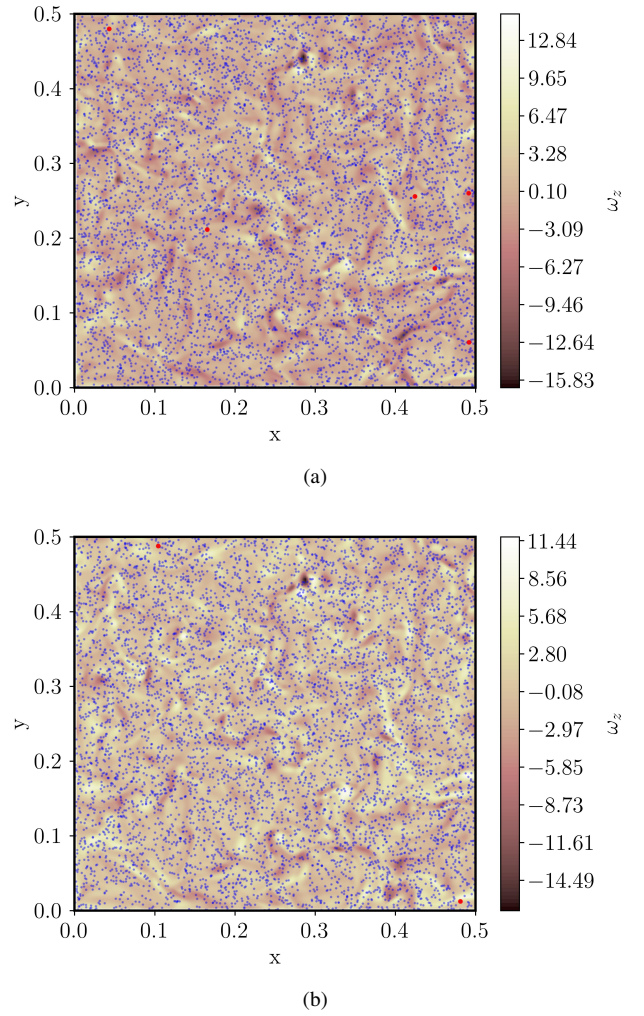


Figure 5: Contour of axial vorticity ω_z on a $x-y$ plane located at $z = 0.4$ for $t/t_\lambda = 4$ with $\alpha = 0.33$ (a) and $\alpha = 1$ (b). MPs are represented by blue dots, and aggregates by red dots.

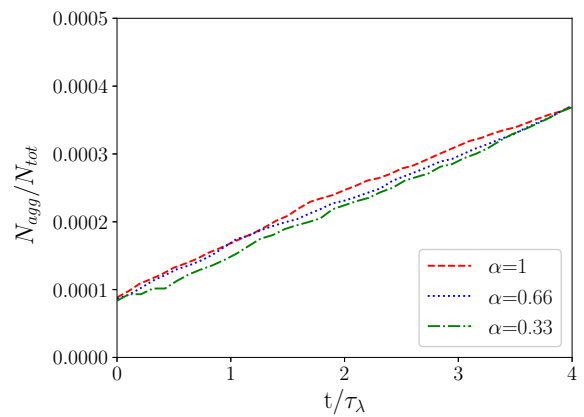


Figure 6: Number of aggregates normalized by the number of total MPs+BPs as a function of time.

α , on marine microplastics in the upper layer of the ocean has been conducted. By simulating two particle classes - microplastics and biogenic particles - in

a setup of homogeneous and isotropic turbulence, it is intended to understand the role of stickiness in particles interaction behavior. In particular, the simulations have revealed that for particles of small size (smaller than the Kolmogorov scale), stickiness does not significantly impact the spatial distribution, and the formation of aggregates. Regardless of the value of α , all cases exhibit typical tracer behavior. Moreover, aggregates formation is rather rare. Therefore, to better observe the effects of coalescence, higher particle number densities or larger particle sizes need to be studied.

Moving forward, next simulation campaigns will incorporate these insights with the ultimate goal of examining the indirect role of biofilm in aggregate formation. The upcoming plans include: (i) to refine the coalescence model towards a more physics-based approach, and (ii) to calibrate the models by means of experimental data.

In conclusion, this preliminary study has provided valuable initial findings regarding the influence of biofilm and stickiness on the distribution and interaction of marine microplastics in turbulent environments.

Acknowledgments

The authors gratefully acknowledge the SRG program (2021-SGR-01045) of the Generalitat de Catalunya (Spain), the *Beatriz Galindo* program (Distinguished Researcher, BGP18/00026) of the Ministerio de Educación y Formación Profesional (Spain), and the computer resources at Cedar provided by the Digital Research Alliance of Canada (RAC-2023 kfw-162-04). Francesco Capuano is a Serra Hünter fellow. C.R.-C. acknowledges the Ramón y Cajal program (RYC2020-029555-I).

Funding sources

This work is funded by the TRITON project (TED2021-132623A-I00) of the *Agencia Estatal de Investigación* (Spain).

References

Balachandar, S. and Eaton, J. K. (2010), Turbulent dispersed multiphase flow, *Annu. Rev. Fluid Mech.*, Vol. 42, pp. 111-133.

Balakin, B. and Hoffmann, A. C. and Kosinski, P. (2012), The collision efficiency in a shear flow, *Chemical Engineering Science*, Vol. 68, pp. 305-312.

Bashir, S. M. and Kimiko, S., and Mak, C-W. and Fang, J.K-H and Goncalves, D. (2021), Personal care and cosmetic products as a potential source of environmental contamination by microplastics in a densely populated Asian city, *Fron. Mar. Sci.*, Vol. 8, pp. 683482.

Clark, J. R. and Cole M. and Lindeque, P. K. and Fileman, E. and Blackford, J and Lewis, C. and Lenton, T. M. and Galloy, T. S. (2016), Marine microplastic debris: a targeted plan for understanding and quantifying interactions with marine life *Front. Ecol. Environ.*, Vol. 14(6), pp. 317-324.

Eerkes-Medrano, D. and Thompson, R. C. and Aldridge, D. C. (2015), Microplastics in freshwater systems: A review of the emerging threats, identification of knowledge gaps and prioritisation of research needs, *Water Research*, Vol. 75, pp. 63-82.

Eriksen, M. and Lebreton, L. C. M. and Carson, H.S. and Thiel, M. and Moore, C. J and Borerro, J. C. and Galgani, F. and Ryan, P. G. and Reisser, J. (2014), Plastic pollution in the World's oceans: more than 5 trillion plastic pieces weighing over 250,000 tons afloat at sea, *PLoS One*, Vol. 9(12), pp. e111913.

Jofre, L. and Papadakis, M. and Roy, P. T. and Aiken, A. and Iaccarino, G. (2020), Multifidelity modeling of irradiated particle-laden turbulence subject to uncertainty, *Int. J. Uncertain Quan.*, vol. 10, pp. 499-514.

Kiorboe, T. and Andersen, K. P and Dam, H. G. (1990), Coagulation efficiency and aggregate formation in marine phytoplankton, *Marine Biology*, vol. 107, pp. 235-245.

Kooi, M. and van Nes, E. H. and Scheffer, M. and Koelmans, A. A. (2017), Ups and downs in the ocean: effects of biofouling on vertical transport of microplastics, *Environ. Sci. Technol.*, Vol. 51(14), pp. 7963-7971.

Michels, J. and Stippkugel, A. and Lenz, M. and Wirtz, K. and Engel, A. (2018), Rapid aggregation of biofilm-covered microplastics with marine biogenic particles, *Proc. R. Soc. Lond. Biol.*, vol. 285(1885), 20181203.

Maxey, M. R. and Riley J. J. (1983), Equation of motion for a small rigid sphere in a nonuniform flow, *Phys. Fluids*, vol. 26, pp. 883-889.

Moreira, J. M. R. and Teodosio, J. S. and Silva, F. C. and Simoes, M. and Melo, L. F. and Mergulhao, F. J. (2013), Influence of flow rate variation on the development of *Escherichia coli* biofilms, *Bioprocess Biosyst Eng.*, vol. 36, pp. 1787-1796.

Pumir, A. and Wilkinson, M. (2016), Collisional aggregation due to turbulence, *Annu. Rev. Condens. Matter Phys.*, Vol. 7, pp. 141-170.

Rahmani, M. and Gupta, A., and Jofre, L. (2022), Aggregation of microplastic and biogenic particles in upper-ocean turbulence, *J. Multiph. Flow*, Vol. 157, pp. 104253.

Subramaniam, S. (2013), Lagrangian–Eulerian methods for multiphase flows, *Prog. Energy Combust.*, vol. 39 (2-3), pp. 215-245.

Takeuchi, M. and Doubell, M. J. and Jackson, G. A. and Yukawa, M. and Sagara, Y. and Yamazaki, H. (2019), Turbulence mediates marine aggregate formation and destruction in the upper ocean, *Nature Research*, vol. 9, pp. 16280.

Teodosio, J. S. and Simoes, M. and Melo, L. F. and Mergulhao, F. J. (2011), Flow cell hydrodynamics and their effects on *E. coli* biofilm formation under different nutrient conditions and turbulent flow, *Biofouling*, vol. 27, pp. 1-11.

van Sebille, E. and Wilcox, C. and Lebreton, L. and Maximenko, N. and Hardesty, B. D. and Franeker, J. A. and Eriksen, M. and Siegel, D. and Galgani, F. and Law, K. L. (2015), A global inventory of small floating plastic debris, *Environ. Res. Lett.*, vol. 10, pp. 124006.